Journal of Medicinal Chemistry

Article

pubs.acs.org/jmc

Discovery, Optimization, and Characterization of Novel D_2 Dopamine Receptor Selective Antagonists

Jingbo Xiao,[†] R. Benjamin Free,[‡] Elena Barnaeva,[†] Jennie L. Conroy,[‡] Trevor Doyle,[‡] Brittney Miller,[‡] Marthe Bryant-Genevier,[†] Mercedes K. Taylor,[†] Xin Hu,[†] Andrés E. Dulcey,[†] Noel Southall,[†] Marc Ferrer,[†] Steve Titus,[†] Wei Zheng,[†] David R. Sibley,[‡] and Juan J. Marugan*[,†]

[†]Discovery Innovation, NIH Chemical Genomics Center, National Center for Advancing Translational Sciences, National Institutes of Health, 9800 Medical Center Drive, Rockville, Maryland 20850, United States

[‡] Molecular Neuropharmacology Section, National Institute of Neurological Disorders and Stroke, National Institutes of Health, 5625 Fishers Lane, Room 4S-04, MSC-9405, Bethesda, Maryland 20892, United States

Supporting Information

ABSTRACT: The D2 dopamine receptor (D2 DAR) is one of the most validated drug targets for neuropsychiatric and endocrine disorders. However, clinically approved drugs targeting D2 DAR display poor selectivity between the D2 and other receptors, especially the D3 DAR. This lack of selectivity may lead to undesirable side effects. Here we describe the chemical and pharmacological characterization of a novel D2 DAR antagonist series with excellent D2 versus D1, D3, D4, and D5 receptor selectivity. The final probe **65** was obtained through a quantitative high-throughput screening campaign, followed by medicinal chemistry optimization, to yield a selective molecule with good in vitro physical properties, metabolic stability, and in vivo pharmacokinetics. The optimized molecule may be a useful in vivo probe for studying D2 DAR signal modulation and could also serve as a lead compound for the development of D2 DAR-selective druglike molecules for the treatment of multiple neuropsychiatric and endocrine disorders.

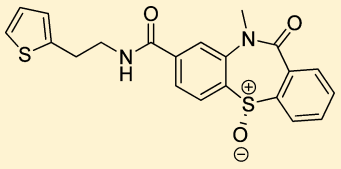

65

Selective D_2 *versus* D_3 antagonist

INTRODUCTION

G-protein-coupled receptors (GPCRs) are among the most intensely investigated drug targets in the pharmaceutical industry.[1] Over 40% of all FDA approved drugs target these important receptor proteins.[2] Unfortunately, many of the ligands that are used as drugs or pharmacological tools are not selective and exhibit some unintended activity on nontarget GPCRs or other proteins.[3] Dopamine receptors (DARs) belong to a large superfamily of neurotransmitter and hormone receptors.[4] Five functionally active DARs have been identified in the mammalian genome.[5] D_1-like DARs (D_1 and D_5) are $G\alpha_s$ coupled, and D_2-like DARs (D_2, D_3, and D_4) are $G\alpha_{i/o}$ coupled.[4,6] There are two isoforms of the D_2 DAR, short and long (D_{2S} and D_{2L}, respectively), which are derived from alternative RNA splicing and vary in the size of their third intracellular loops. The D_{2L} isoform is more prevalent, although both isoforms appear to be functionally similar.[7] Among the DARs, the D_2 DAR is arguably one of the most validated drug targets in neurology and psychiatry. For instance, all receptor-based antiparkinsonian drugs work via stimulating the D_2 DAR (although controversy exists for a minor role of the D_1 DAR), whereas all FDA approved antipsychotic agents are antagonists of this receptor.[8] The D_2 DAR is also therapeutically targeted in other disorders such as restless legs syndrome, tardive dyskinesia, Tourette's syndrome, and hyperprolactinemia. Most drugs targeting the D_2 DAR (orthosteric agonists and antagonists) are problematic by being less efficacious than desired or possessing limiting side effects, most of which are due to off-target cross-GPCR reactivity.[9] It would thus be desirable to develop a class of novel therapeutic agents with higher selectivity for the D_2 DAR.

It should be noted that although the therapeutic potential for more selective D_2 DAR antagonists may be enormous, this approach may also provide a way forward for developing selective pharmacological probes that provide a better understanding of the dopamine neurocircuitry. Among the D_2-like family of DARs (D_2, D_3, and D_4), only the D_4 DAR has ligands (both agonists and antagonists) that are truly specific versus D_2 and D_3 DARs.[10] This is not surprising given that the D_4 DAR is more structurally divergent compared to the D_2/D_3 DARs. D_2 and D_3 receptors share 78% homology in their transmembrane spanning domains, which harbor the ligand binding sites, and thus, the pharmacologic properties between these two receptor subtypes are quite similar.[4,11] Therefore, it is very challenging to identify small molecules that can selectively bind to and/or functionally modulate either D_2 or D_3 DAR receptor subtypes. With respect to the D_3 DAR, there are several compounds that exhibit good selectivity versus the D_4 DAR and moderate−high selectivity versus the D_2 DAR.[12] Some of these D_3-selective compounds have been used for in vivo experiments, but the results have been controversial in many instances.[13] In contrast, to the best of our knowledge, there are only a few series of compounds that exhibit even moderate selectivity for the D_2

Received: January 23, 2014
Published: March 25, 2014

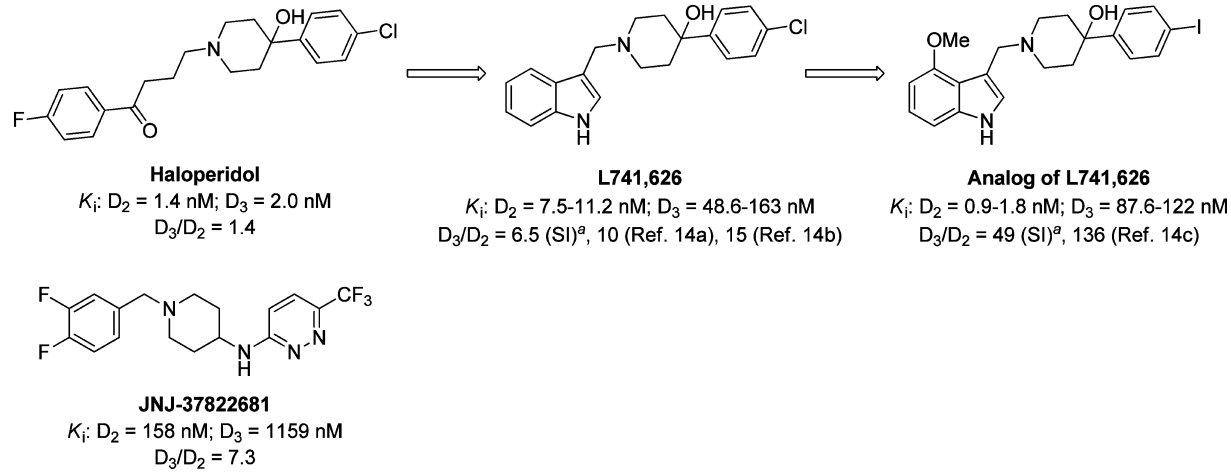

Figure 1. Known chemical series of selective D_2 versus D_3 DAR antagonists. Superscript "a" indicates that additional information is in Table S15 in Supporting Information.

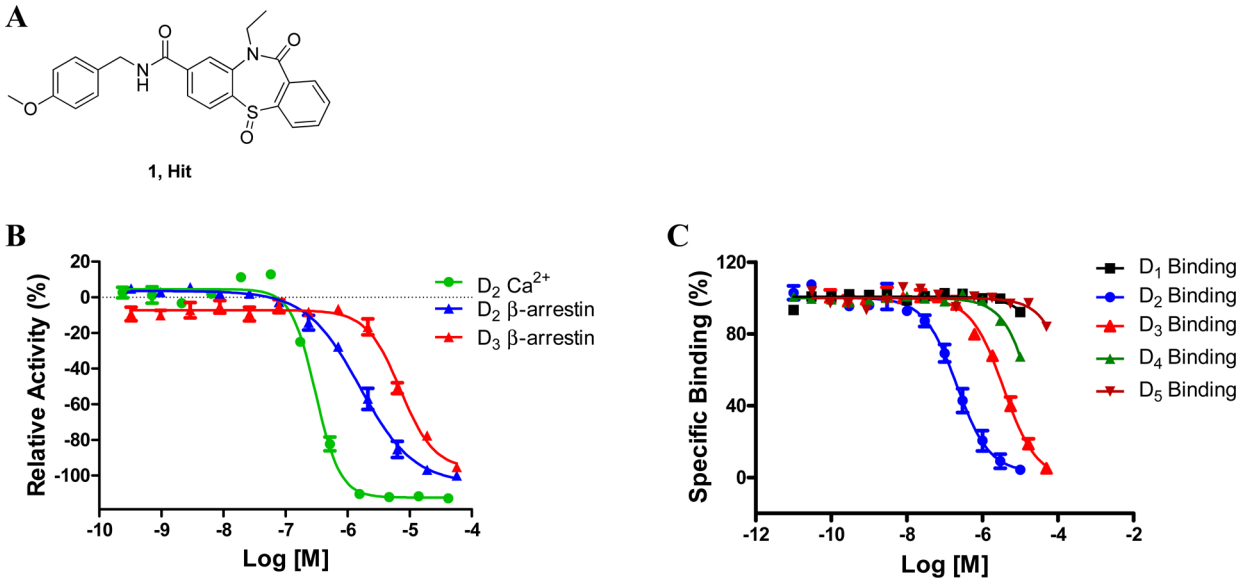

Figure 2. (A) Structure of the hit compound **1**. (B) Graphical representation of the dose–response curves of **1** in D_2 Ca^{2+} assay (green, AC_{50} = 0.280 ± 0.012 μM), D_2 β-arrestin assay (blue, AC_{50} = 2.89 ± 0.25 μM), and D_3 β-arrestin assay (red, AC_{50} = 5.76 ± 1.18 μM). (C) Graphical representation of the dose–response curves of **1** in binding assays for D_1 (black), D_2 (blue, K_i = 0.30 ± 0.09 μM), D_3 (red, K_i = 1.9 ± 0.9 μM), D_4 (green), and D_5 (brown).

DAR receptor versus the D_3 and D_4 DARs within the D_2-like DAR subfamily (Figure 1).[14] Selective antagonists of the D_2 DAR could be useful for the therapy of disorders currently treated with relatively nonselective D_2 blockers, including Tourette's syndrome, tardive dyskinesia, Huntington's chorea, and schizophrenia. Probably the biggest impact, in terms of patient population, would be in the treatment of schizophrenia.

Here, we present a novel series of selective small molecule antagonists of D_2 DAR identified from a quantitative high-throughput screening (qHTS) campaign.[14] Optimized lead compounds in this series, represented by **65**, exhibit excellent D_2 versus D_3 and D_4 DAR selectivity in addition to good ADME and in vivo pharmacokinetics properties, which make them good pharmacological tools to perform proof-of-concept studies using animal models as well as for further development into druglike molecules.

RESULTS AND DISCUSSION

The primary goal of this project was to identify and develop novel small molecule modulators of the D_2 DAR with selectivity versus the D_3 DAR for use as in vitro and in vivo pharmacological tools and in proof-of-concept experiments in animal models of neuropsychiatric disease. To this end, we performed a full qHTS campaign of ~380 000 molecules of the NIH Molecular Libraries Small Molecule Repository (MLSMR). For the initial qHTS screen, we employed a calcium release assay where cellular coexpression of the D_2 DAR with a chimeric G_{qi5} protein enabled the receptor to stimulate Ca^{2+} mobilization, which was detected through the excitation of an intracellular fluorescent dye. The hit compounds were orthogonally validated using a D_2 DAR β-arrestin assay (DiscoveRx) and counterscreened using the same β-arrestin assay but with the D_3 DAR. Compounds that showed selectivity for D_2 versus D_3 receptors were further characterized using radioligand binding assays, and K_i values were determined

dx.doi.org/10.1021/jm500126s | J. Med. Chem. 2014, 57, 3450–3463

Scheme 1. General Synthetic Route for Analogues Shown in Tables 1−3

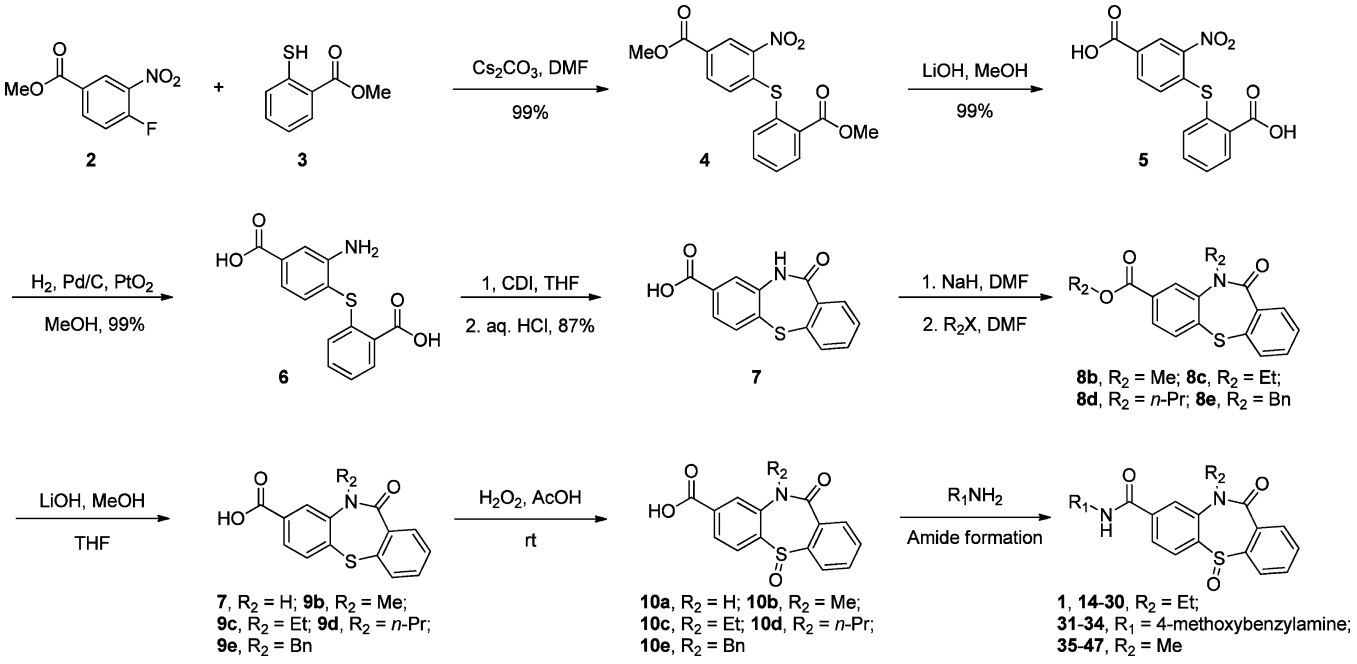

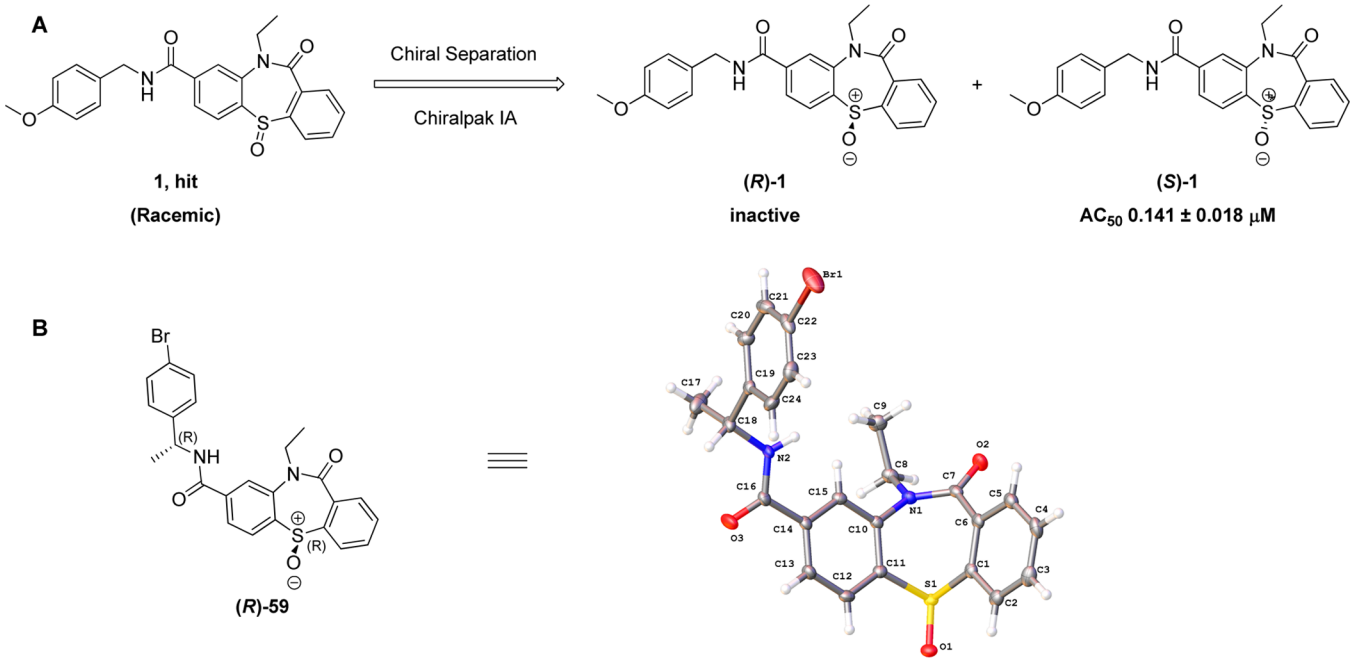

Figure 3. (A) Preparative chiral HPLC separation of the original racemic hit **1** and absolute stereochemistry assignment. (B) Single crystal X-ray structure of the inactive enantiomer ((*R*)-**59**).

for each receptor subtype. While multiple modulator chemotypes were identified within this qHTS project, we specifically focused here on the identification of a novel antagonist with selectivity for the D_2 receptor. From the primary screen, 2294 compounds were identified with D_2 DAR antagonist activity, although 858 of these were not subsequently confirmed. Of the remaining, 499 compounds were selected for counterscreening against the D_3 DAR as described above. Several compounds were identified that exhibited D_2 versus D_3 DAR selectivity with the most promising hit compounds being selected for chemical optimization.

The hit compound **1** (Figure 2A), initially identified from pilot screens for the project, displayed selectivity for the D_2 versus the D_3 DAR in a functional assay (Figure 2B) and selectivity versus other DAR subtypes in radioligand binding assays (Figure 2C). This molecule bears a benzothiazepine moiety, a chemical scaffold that is often capable of crossing the blood−brain barrier (BBB).[15] In addition, an interesting aspect of this scaffold is the lack of basic nitrogen. Almost all known compounds with affinity to dopaminergic receptors contain a basic nitrogen in the structure. The lack thereof in this structural class would thus be of interest to the scientific community. Furthermore, this molecule has promising physical

dx.doi.org/10.1021/jm500126s | J. Med. Chem. 2014, 57, 3450−3463

Scheme 2. General Synthetic Routes (A) for Analogues Shown in Table 4, (B) for Analogues Shown in Table 5, and (C) for Analogues Shown in Table 6

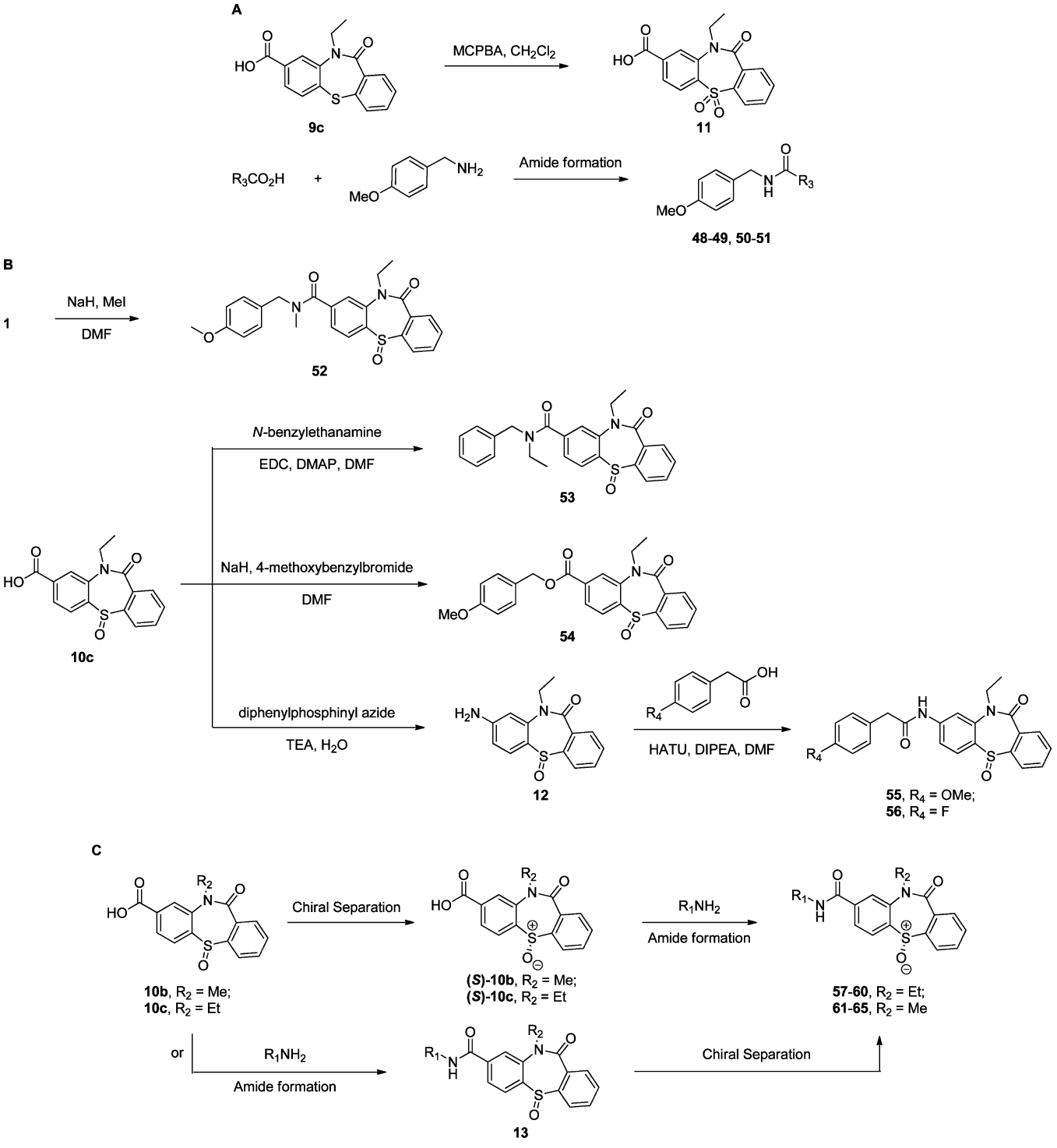

properties rendering it a candidate for further optimization. Importantly, in functional assays the molecule clearly demonstrated receptor selectivity, and therefore, we decided to pursue SAR studies with this molecule to identify improved D_2-receptor selective probes, specifically focusing on D_2 versus D_3 receptor selectivity.

In order to identify both potent and selective D_2 antagonists, we employed a two-stage development plan. In the first stage we used a D_2 DAR Ca^{2+} mobilization assay to drive our SAR study identifying potent D_2 antagonists. Optimized analogues with good potency were further characterized for receptor selectivity in the second stage using D_2 and D_3 β-arrestin activation functional assays, as well as direct radioligand binding assays.

According to our general practice, we started our medicinal chemistry campaign with a resynthesis of the original hit **1** (Scheme 1).[16] The activity of the synthesized material was reconfirmed with slightly better potency than that of the

dx.doi.org/10.1021/jm500126s | J. Med. Chem. 2014, 57, 3450−3463

Table 1. SAR with Modifications on the Benzyl Moiety[a]

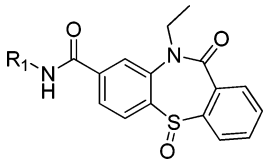

Entry	R_1	Ca^{2+} AC_{50} (μM)	Entry	R_1	Ca^{2+} AC_{50} (μM)
1	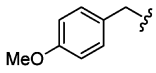	0.280 ± 0.012	22	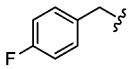	0.089 ± 0.009
14	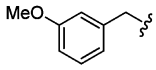	0.112 ± 0.030	23	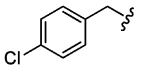	0.509 ± 0.251
15	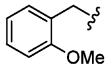	4.46 ±1.46	24	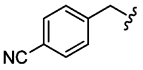	0.141 ± 0.026
16	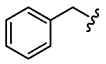	0.445 ± 0.104	25	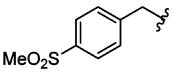	0.353 ± 0.059
17	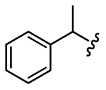	0.560 ± 0.047	26	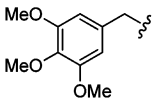	1.77 ± 0.09
18	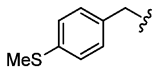	0.223 ± 0.026	27	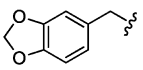	0.353 ± 0.068
19	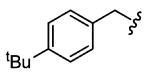	0.353 ± 0.132	28		0.887 ± 0.155
20	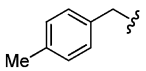	0.177 ± 0.042	29	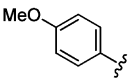	0.141 ± 0.025
21	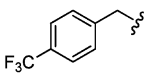	0.141 ± 0.027	30	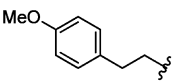	0.353 ± 0.061

[a] AC_{50} ± SEM (n = 3) is from a calcium accumulation assay.

original qHTS sample (AC_{50} = 0.280 μM versus 0.560 μM for the qHTS sample). As the hit compound **1** represents a racemic mixture, both *R*- and *S*-enantiomers were obtained from preparative chiral HPLC separation of racemic material. Interestingly, when the enantiomerically pure samples were evaluated, only one isomer showed activity and, as expected, had twice the potency than the racemic material. The other enantiomer was inactive up to 77 μM (Figure 3A). In order to assign the absolute stereochemistry of the active enantiomer, a pair of analogues bearing a known second chiral center (*R*-) and a heavy atom (Br) were prepared. Fortunately, a single crystal was obtained for the inactive enantiomer of this pair of molecules. X-ray diffraction analysis was successfully performed disclosing that the inactive isomer ((*R*)-**59**) had the 5-oxide as the *R*-configuration (Figure 3B). Therefore, we concluded that the active enantiomer has an *S*-configuration within the sulfoxide functional group.

With these promising results in hand, we decided to initiate our medicinal chemistry SAR studies with the aim of evaluating several distinct areas of the molecule. The synthesis of analogues is shown in Scheme 1 and Scheme 2. A S_NAr reaction between methyl 4-fluoro-3-nitrobenzoate (**2**) and methyl 2-mercaptobenzoate (**3**) gave intermediate **4** which was saponificated with LiOH to offer the acid **5**. The nitro functional group was reduced using H_2 and a mixed catalyst of 10% palladium on carbon and platinum oxide to produce the amine **6**. The intramolecular cyclization was induced by CDI to provide the benzothiazepine **7**. Alkylation of the nitrogen of the amide or the oxygen of the acid with a variety of alkyl halides gave intermediate **8**. Selective hydrolysis of esters motif provided the 8-carboxylic acid substituted benzothiazepine **9**. Thioester mono-oxidation with hydrogen peroxide yields sulfoxides **10** which were coupled with different amines to offer the final products as shown in Scheme 1. Additionally, thioester **9c** can be overoxidized with MCPBA to produce the sulfone **11** (Scheme 2A). Curtius rearrangement of the carboxylic acid **10c** with diphenylphosphinylazide provides the 8-amino substituted benzothiazepine **12** as a key intermediate for the synthesis of reverse amide analogues **55** and **56** (Scheme 2B). The enantiomerically pure analogues can be prepared using two routes alternating the chiral separation and the amide formation as it is shown in Scheme 2C.

A summary of our medicinal chemistry SAR efforts to improve the potency of the compounds is disclosed in Tables 1−6. As an initial approach, we conducted this study using racemic mixtures. The first area evaluated was the 4-

dx.doi.org/10.1021/jm500126s | J. Med. Chem. 2014, 57, 3450−3463

methoxybenzyl moiety of the molecule starting with the systematic replacement of functional groups around the benzyl ring. In doing so, the benzothiazepine moiety and amide linker were held constant while the substitution pattern and steric and electronic effects of the substituents were fully explored, as shown in Table 1. It can be seen that the *o*-methoxy substituent was not well tolerated producing a considerable loss of potency (**15**, AC_{50} = 4.46 μM), while the *m*-methoxy substitution resulted in an analogue with slightly improved potency (**14**, AC_{50} = 0.112 μM). Removal of all functionality within the benzyl ring (**16**, AC_{50} = 0.445 μM) or addition of one methyl substituent in the α-methylene functional group (**17**, AC_{50} = 0.560 μM) yielded analogues with 2 times lower potencies than that of the original hit (**1**, AC_{50} = 0.280 μM). Interestingly, neither the electronic nor the steric nature of para substituents had a significant effect on the activity, as many of them were generally well tolerated (**18**−**25**, AC_{50} = 0.089−0.509 μM), with the 4-fluoro compound (**22**, AC_{50} = 0.089 μM) being the most potent analogue. Multisubstituted analogue **26** showed a 6-fold decrease of potency (AC_{50} = 1.77 μM). Cyclization of the 3,4-disubstituted methoxy groups restored the activity (**27**, AC_{50} = 0.353 μM). Both removal of a methylene spacer functional group (phenyl, **28** and **29**) and inclusion of an additional methylene functional group (phenylethylene, **30**) were well tolerated, although the effect was dependent on the substitution on the aromatic ring (**1** versus **29**; **16** versus **28**).

In parallel to systematic SAR studies of the 4-methoxybenzyl functional group, we investigated the effect of substituents within the benzothiazepine amide moiety, as detailed in Table 2. Total removal of the ethyl group led to a loss in activity (**31**, AC_{50} = 0.887 μM). Analogue **32** with methyl substitution gave a 2.5-fold activity increase. Moreover, the size of the substituent decreased potency (methyl, **32**, AC_{50} = 0.112 μM; ethyl, **1**, AC_{50} = 0.280 μM; *n*-propyl, **33**, AC_{50} = 0.705 μM; benzyl, **34**, AC_{50} = 8.87 μM). In light of the methyl group being the most promising substituent for R_2, additional analogues that carried a methyl group as the substituent on the benzoazepine amide are detailed in Table 3. Other than substituted phenyl and benzyl rings (**35**−**41**), heteroaryl (**42**−**44**), heterocyclic (**45** and **46**), and aliphatic (**47**) groups were also evaluated. Most of R_1 substituents listed in Table 3 were well tolerated except analogue **42** containing a 2-pyridylmethyl group. Several potent analogues with an AC_{50} of less than 0.1 μM were identified from this round of SAR investigation (**41**, AC_{50} = 0.071 μM; **44**, AC_{50} = 0.089 μM; **45**, AC_{50} = 0.089 μM). It was interesting to note that activity of analogue **36** with a 4-methoxyphenyl group was >4-fold more active than the corresponding analogue **35** with a plain phenyl group.

Table 2. SAR with Modifications on the Benzothiazepine Amide Moiety[a]

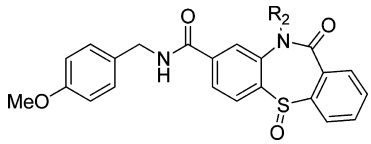

compd	R_2	Ca^{2+}, AC_{50} (μM)
31	H	0.887 ± 0.221
32	Me	0.112 ± 0.025
33	*n*-Pr	0.705 ± 0.413
34	Bn	8.87 ± 1.39

[a]AC_{50} ± SEM (n = 3) is from a calcium accumulation assay.

With several improved analogues in hand, SAR studies were focused on replacements within the benzothiazepine core, as shown in Table 4. Replacement of the sulfoxide by a thioether functional group resulted in a 2.5-fold reduction of activity (**48**, AC_{50} = 0.705 μM). Importantly, the corresponding sulfone analogue was completely inactive (**49**), in line with our previous observation that only the enantiomer ((*S*)-**1**, AC_{50} = 0.141 μM) with *S*-configuration displays antagonism and the analogue (*R*)-**1** with *R*-configuration is totally inactive. Other three-ring system replacements, such as anthracene-9,10-dione or 2-phenylisoindoline-1,3-dione, led to a complete loss of activity (**50** and **51**, inactive).

Next, we examined different linkers as replacement for the amide functionality as detailed in Table 5. Alkylation of the N−H led to a complete or major loss in activity (**52**, inactive; **53**, AC_{50} = 56.0 μM). Switching of the amide moiety to an ester group eliminated any activity (**54**, inactive). Analogues with a reversed amide moiety were also tolerated displaying reasonable activity (**55**, AC_{50} = 0.705 μM; **56**, AC_{50} = 0.223 μM). After investigation of SAR in all the previously described areas, a clear SAR picture of this chemical scaffold was developed and is summarized in Figure 4.

Lastly, 10 selected analogues were subjected to preparative chiral HPLC in order to obtain enantiomerically pure analogues for further evaluation and profiling. The activity of the 10 active enantiomers (*S*-configuration) is listed in Table 6. Most of the analogues in this table showed AC_{50} values lower than 300 nM. As we expected, the corresponding chiral versions of the three most potent racemic analogues (**41**, **44**, and **45** in Table 3) were still ranked as the top three most potent analogues (**62**, AC_{50} = 0.089 μM; **64**, AC_{50} = 0.070 μM; **65**, AC_{50} = 0.070 μM). For further confirmation of the absolutely stereochemistry of our most active compounds a single crystal X-ray structure of **65** was successfully obtained resulting in the expected *S*-configuration (Figure 5).

In addition to the activity in the D_2 Ca^{2+} assay, these chiral analogues were profiled for D_2/D_3 receptor selectivity along with the original hit **1**, the racemic mixture of the probe molecule **44** (*rac*-**65**), and its separated inactive *R*-configuration analogue (*R*)-**65** (Table 7). Because of the lack of a D_3 DAR stably transfected cell line with which to activate the chimeric G-protein (G_{qi5}) Ca^{2+} pathway, we used cell lines designed to interrogate the β-arrestin pathway to evaluate the D_2/D_3 functional selectivity. Overall, antagonistic activities in the D_2 Ca^{2+} assay correlated quite well with those observed in the D_2 β-arrestin assay; however, a ∼10-fold potency shift between two assays was noted. The selectivity between D_2 and D_3 β-arrestin assays ranged from 2.0- to 22.3-fold. In addition to the comparison of functional selectivities in β-arrestin assay, we further evaluated the D_2/D_3 receptor binding selectivity using a radioligand displacement assay to determine the K_i values of the compounds. While we did observe some differences in fold selectivity between the two methods (possibly due to different error rates inherent in calculating both values and potential small differences in functional selectivity among analogues), all compounds showed D_2 DAR selectivity and the lead analogues, including **44** and **65**, consistently displayed greater than 17-fold selectivity for the D_2 DAR using both β-arrestin and radioligand binding assays. Specifically, by use of radioligand binding, which directly measures the affinity of test compound for the receptors, analogue **65** displayed 41-fold selectivity for the D_2

dx.doi.org/10.1021/jm500126s | J. Med. Chem. 2014, 57, 3450−3463

Table 3. SAR with Combined Modifications on the Benzyl Moiety and Benzothiazepine Amide Moiety[a]

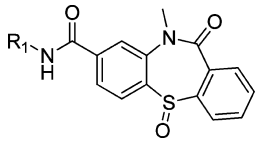

Entry	R_1	Ca^{2+} AC_{50} (μM)	Entry	R_1	Ca^{2+} AC_{50} (μM)
35		1.58 ± 0.17	**42**	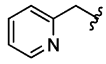	11.2 ± 4.6
36	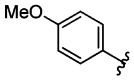	0.353 ± 0.102	**43**	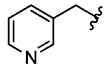	0.281 ± 0.034
37	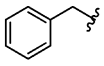	0.223 ± 0.028	**44**	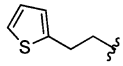	0.089 ± 0.020
38	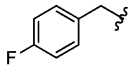	0.353 ± 0.138	**45**	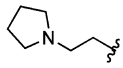	0.089 ± 0.015
39	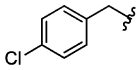	0.141 ± 0.041	**46**	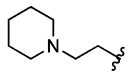	0.112 ± 0.017
40	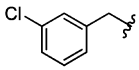	0.281 ± 0.072	**47**	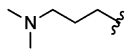	0.560 ± 0.165
41	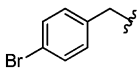	0.071 ± 0.004			

[a]AC_{50} ± SEM (n = 3) is from a calcium accumulation assay.

Table 4. SAR with Modifications on the Benzothiazepine[a]

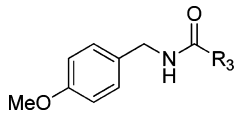

Entry	R_3	Ca^{2+} AC_{50} (μM)	Entry	R_3	Ca^{2+} AC_{50} (μM)
48	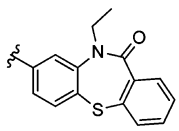	0.705 ± 0.366	**(*R*)-1**	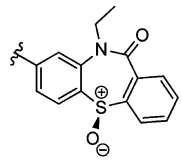	> 77
49	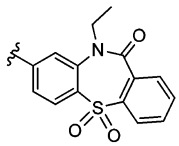	> 77	**50**	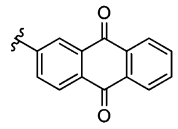	> 77
(*S*)-1	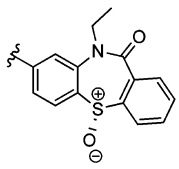	0.141 ± 0.018	**51**	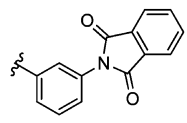	> 77

[a]AC_{50} ± SEM (n = 3) is from a calcium accumulation assay.

versus the D_3 receptor (Table 7 and Supporting Information Table S15 for comparison to reference compounds). This compound could thus be used to substantially block the D_2 receptor in vivo with minimal effects on the D_3 receptor.

dx.doi.org/10.1021/jm500126s | J. Med. Chem. 2014, 57, 3450−3463

Table 5. SAR with Modifications on the Left Amide Linker[a]

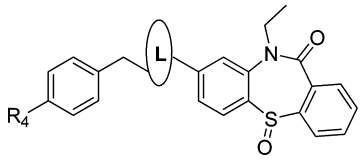

Entry	R_4	L (Linker)	Ca^{2+} AC_{50} (μM)
52	OMe		> 77
53	H		56.0 ± 16.6
54	OMe		> 77
55	OMe		0.705 ± 0.112
56	F		0.223 ±0.099

[a] AC_{50} ± SEM (n = 3) is from a calcium accumulation assay.

Considering ligand potency and D_2/D_3 selectivity, as determined using β-arrestin functional assays and radioligand binding assays, we chose analogue **65** for further in vitro metabolic profile and in vivo mouse pharmacokinetics (PK) studies. As shown in Table 8, analogue **65** demonstrated excellent PBS aqueous buffer solubility (113.3 μM), good mouse and human liver microsomal stability with a very reasonable intrinsic half-lives ($T_{1/2}$ of 24.7 and 26.4 min, respectively), promising mouse and human plasma stability, and good cell permeability. Overall, analogue **65** has an excellent metabolic profile and physical properties. Therefore, analogue **65** was further evaluated using C57BL/6 mice for in vivo pharmacokinetics (PK) studies to investigate the organ distribution of this compound in plasma and brain using an intraperitoneal (ip) single dose administration of 30 mg/kg (Figure 6). Analogue **65** displays a plasma half-life of 1.67 h with a similar value in brain ($T_{1/2}$ = 1.30 h), demonstrating also acceptable blood–brain barrier (BBB) penetration. The brain to plasma ratio was found to be 0.181. The concentration of analogue **65** in brain reached 4.19 μmol/kg (C_{max}) within 15 min. Further in vivo studies, including the displacement of radiotracers, are warranted for confirmation of this activity.

CONCLUSION

In summary, analogue **65** displays the best combination of overall activity, improved potency, and good physical properties. Furthermore, the excellent selectivity between D_2 and D_3 receptors coupled with a promising ADME profile (Table 8) and encouraging in vivo pharmacokinetics properties (Figure 6, Supporting Information) led us to declare the lead compound **65** as a selective D_2/D_3 DAR antagonist.

EXPERIMENTAL SECTION

a. Chemistry. All air or moisture sensitive reactions were performed under positive pressure of nitrogen with oven-dried glassware. Anhydrous solvents such as dichloromethane, *N*,*N*-dimethylformamide (DMF), acetonitrile, methanol, and triethylamine were purchased from Sigma-Aldrich (St. Louis, MO). Preparative

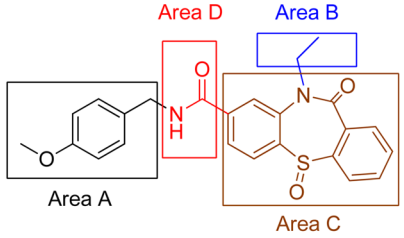

Area A: *Ortho*-substituents are not tolerated. Both the electronic and steric nature of substituents don't have a significant effect on the activity, as many substituents are generally well tolerated at *para*-position. Certain heterocycles or alphatic chains are also tolerated.

Area B: Other than proton, as the size increases the potency decreases (H < Me > Et > *n*-Pr > Bn).

Area C: Only the *S*-enantiomer is active (*S*-sulfoxide > thio >> *R*-sulfoxide, sulfone, and other 3-ring systems). It suggests that benzoazepine ring has a direct interaction with the receptor.

Area D: Free N-H is necessary for the actvity. Reversed amides are also tolerated. Data suggests that the N-H in this amide moiety could participate in a hydrogen bond interaction with the receptor.

Figure 4. SAR summary.

dx.doi.org/10.1021/jm500126s | J. Med. Chem. 2014, 57, 3450–3463

Table 6. Enantiomerically Pure Version of Selected Analogues[a]

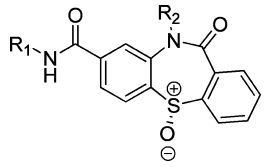

Entry	R_2	R_1	Ca^{2+} AC_{50} (μM)	Entry	R_2	R_1	Ca^{2+} AC_{50} (μM)
(*S*)-1	Et	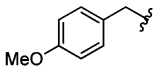	0.141 ± 0.018	**61**	Me	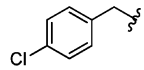	0.280 ± 0.053
57	Et	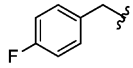	0.056 ± 0.006	**62**	Me	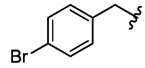	0.089 ± 0.016
58	Et	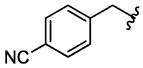	0.112 ± 0.032	**63**	Me	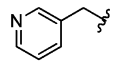	0.445 ± 0.085
59	Et	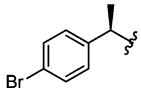	0.223 ± 0.050	**64**	Me	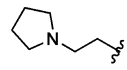	0.070 ± 0.017
60	Et	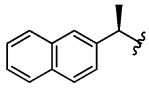	0.353 ± 0.067	**65**	Me	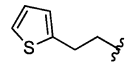	0.070 ±0.014

[a]AC_{50} ± SEM (n = 3) is from a calcium accumulation assay.

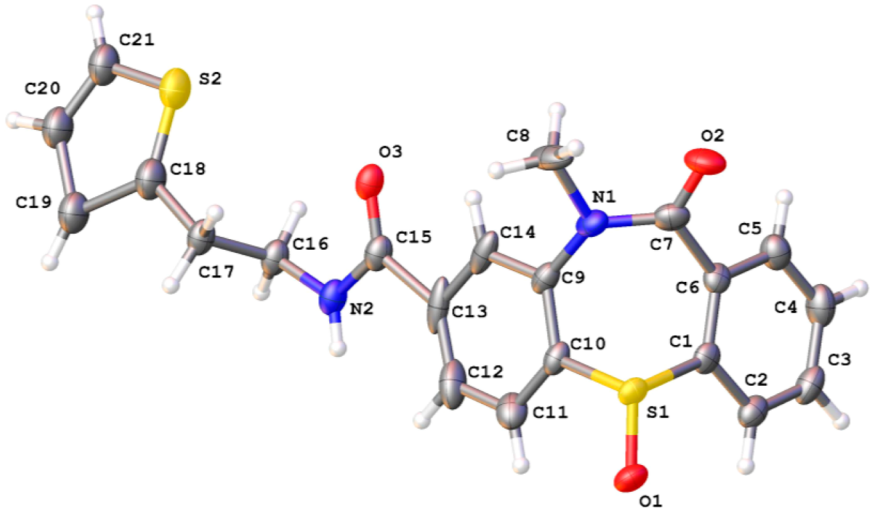

Figure 5. X-ray crystal structure of **65**. X-ray parameters are listed in the Supporting Information.

purification was performed on a Waters semipreparative HPLC system (Waters Corp., Milford, MA). The column used was a Phenomenex Luna C_{18} (5 μm, 30 mm × 75 mm; Phenomenex, Inc., Torrance, CA) at a flow rate of 45.0 mL/min. The mobile phase consisted of acetonitrile and water (each containing 0.1% trifluoroacetic acid). A gradient of 10−50% acetonitrile over 8 min was used during the purification. Fraction collection was triggered by UV detection at 220 nM. Analytical analysis was performed on an Agilent LC/MS (Agilent Technologies, Santa Clara, CA). Method 1 consisted of the following: a 7 min gradient of 4−100% acetonitrile (containing 0.025% trifluoroacetic acid) in water (containing 0.05% trifluoroacetic acid) was used with an 8 min run time at a flow rate of 1.0 mL/min. Method 2 consisted of the following: a 3 min gradient of 4−100% acetonitrile (containing 0.025% trifluoroacetic acid) in water (containing 0.05% trifluoroacetic acid) was used with a 4.5 min run time at a flow rate of 1.0 mL/min. A Phenomenex Luna C_{18} column (3 μm, 3 mm × 75 mm) was used at a temperature of 50 °C. Purity determination was performed using an Agilent diode array detector for both method 1 and method 2. Mass determination was performed using an Agilent 6130 mass spectrometer with electrospray ionization in the positive mode. ^{1}H NMR spectra were recorded on Varian 400 MHz spectrometers (Agilent Technologies, Santa Clara, CA). Chemical shifts are reported in ppm with undeuterated solvent (DMSO at 2.49 ppm) as internal standard for DMSO-d_6 solutions. All of the analogues tested in the biological assays have a purity of greater than 95% based on both analytical methods. High resolution mass spectra were recorded on Agilent 6210 time-of-flight (TOF) LCMS system. Confirmation of molecular formula was accomplished using electrospray ionization in the positive mode with the Agilent Masshunter software (version B.02).

dx.doi.org/10.1021/jm500126s | J. Med. Chem. 2014, 57, 3450−3463

Table 7. Selectivity Profiling of D_2 versus D_3 for 13 Selected Analogues[a]

Entry	D_2 Ca^{2+} AC_{50} (μM)	D_2 β-arrestin AC_{50} (μM)	D_3 β-arrestin AC_{50} (μM)	D_2 K_i (μM)	D_3 K_i (μM)	D_3/D_2 (β-arrestin)	D_3/D_2 (K_i)
1	0.280 ± 0.012	2.89 ± 0.25	5.76 ± 1.18	0.30 ± 0.09	1.9 ± 0.9	2.0	6.3
(*S*)-1	0.141 ± 0.018	1.15 ± 0.16	2.89 ± 1.21	N/A	N/A	2.5	N/A
57	0.056 ± 0.006	0.576 ± 0.036	3.24 ± 0.18	0.090*	0.23*	5.6	2.6
58	0.112 ± 0.32	0.257 ± 0.014	1.62 ± 0.10	0.023*	0.13*	6.3	5.7
59	0.223 ± 0.050	1.29 ± 0.070	9.13 ± 1.74	0.53 ± 0.16	0.88*	7.1	1.7
60	0.353 ± 0.067	2.89 ± 0.272	32.4 ± 12.1	0.29 ± 0.10	3.4 ± 0.8	11.2	11.7
61	0.280 ± 0.053	2.89 ± 0.203	10.2 ± 3.0	N/A	N/A	4.5	N/A
62	0.089 ± 0.016	1.02 ± 0.265	4.57 ± 0.25	0.24*	0.37*	4.5	1.5
63	0.445 ± 0.085	2.89 ± 0.203	14.5 ± 3.0	0.31*	21.0*	5.0	70.0
64	0.070 ± 0.017	0.363 ± 0.022	4.57 ± 0.62	0.21*	0.35*	12.6	1.7
44	0.089 ± 0.020	0.913 ± 0.287	20.4 ± 6.0	0.19 ± 0.04	9.2 ± 1.7	22.3	48.4
***Rac*-65**							
(*R*)-65	> 77	> 77	> 77	> 50	> 50	N/A	N/A
65	0.070 ± 0.014	0.725 ± 0.113	12.9 ± 3.2	0.10 ± 0.01	4.1 ± 0.8	17.8	41.0

[a]Blue columns are for D_2 receptor, and red columns are for D_3 receptor. The asterisk (*) indicates a value without error and that the curve is provided in the Supporting Information.

Table 8. Comparison of Physical and Metabolic Properties for Hit Compound 1 and Lead Compound 65

	aqueous kinetic solubility		liver microsomal stability ($T_{1/2}$ in min)		plasma stability (% remaining after 2 h)		Caco-2 permeability (10^{-6}, cm/s)	
compd	μg/mL	μM	mouse	human	mouse	human	$P_{app(A-B)}$	$P_{app(B-A)}$
1	11.5	26.4	35.9	N/A	N/A	N/A	21.6	16.2
65	46.5	113.3	24.7	26.4	95.2	98.4	18.8	23.8

*Detailed Preparation Procedure for **65** Is Described Below. Methyl 4-(2-(Methoxycarbonyl)phenylthio)-3-nitrobenzoate (**4**).* A solution of methyl 4-fluoro-3-nitrobenzoate (**2**, 12.1 g, 60.9 mmol) and methyl 2-mercaptobenzoate (**3**, 9.21 mL, 66.9 mmol) in DMF (6.00 mL) was treated with Cs_2CO_3 (19.8 g, 60.9 mmol) at room temperature. The reaction mixture was stirred at 40 °C for 4 h and then cooled to room temperature. Ice−water was added to induce the precipitation. The precipitate was filtered, washed with water, and dried to give 21.0 g (99%) of the title compound as a yellow solid which was used directly in the next reaction without further purification. ^{1}H NMR (400 MHz, DMSO-d_6) δ ppm 8.63 (d, J = 2.0 Hz, 1 H), 8.04 (dd, J = 8.4, 1.8 Hz, 1 H), 7.87−7.99 (m, 1 H), 7.57−7.77 (m, 3 H), 7.05 (d, J = 8.6 Hz, 1 H), 3.88 (s, 3 H), 3.71 (s, 3 H); LCMS t_R = 6.19 min, m/z 365.0 [M + Na^+]; HRMS (ESI) m/z calcd for $C_{16}H_{13}NNaO_6S$ [M + Na^+] 371.0387, found 371.0393.

*4-(2-Carboxyphenylthio)-3-nitrobenzoic Acid (**5**).* A solution of methyl 4-(2-(methoxycarbonyl)phenylthio)-3-nitrobenzoate (**4**, 21.0 g, 60.5 mmol) in THF (150 mL) and water (150 mL) was treated at room temperature with LiOH (14.5 g, 605 mmol). The reaction mixture was stirred at 60 °C for 2 h. The organic solvent was removed and the aqueous solution was washed with EtOAc and acidified with 2 N HCl until pH ≈ 2. The yellow precipitate was filtered, washed with water, and dried to give 19.1 g (99%) of the title compound as a yellow solid which was used directly in the next reaction without further purification. ^{1}H NMR (400 MHz, DMSO-d_6) δ ppm 13.53 (br s, 1 H), 13.27 (br s, 1 H), 8.58 (d, J = 1.6 Hz, 1 H), 8.01 (dd, J = 8.6, 2.0 Hz, 1 H), 7.85−7.95 (m, 1 H), 7.48−7.68 (m, 3 H), 7.07 (d, J = 8.6 Hz, 1 H); LCMS t_R = 4.73 min, m/z 341.9 [M + Na^+]; HRMS (ESI) m/z calcd for $C_{14}H_9NNaO_6S$ [M + Na^+] 342.0043, found 342.0047.

*3-Amino-4-(2-carboxyphenylthio)benzoic Acid (**6**).* A solution of 4-(2-carboxyphenylthio)-3-nitrobenzoic acid (**5**, 8.70 g, 27.2 mmol) in MeOH (300 mL) was treated at room temperature with platinum(IV) oxide (300 mg, 1.32 mmol) and Pd/C (10%, 600 mg, 5.64 mmol). A balloon containing H_2 was connected to the flask, and the reaction flask was repeatedly evacuated and refilled with H_2. After 16 h, additional Pd/C (10%, 600 mg, 5.64 mmol) was added and the reaction mixture was stirred under H_2 balloon for an additional 32 h. The reaction mixture was filtered through a pad of Celite and concentrated to give 7.80 g (99%) of the title compound as a gray-yellow solid which was used directly in the next reaction without further purification. ^{1}H NMR (400 MHz, DMSO-d_6) δ ppm 12.99 (br s, 2 H), 7.92 (dd, J = 7.8, 1.6 Hz, 1 H), 7.42 (d, J = 1.6 Hz, 1 H), 7.37 (d, J = 7.8 Hz, 1 H), 7.31−7.36 (m, 1 H), 7.18 (td, J = 7.6, 1.2 Hz, 1

dx.doi.org/10.1021/jm500126s | J. Med. Chem. 2014, 57, 3450−3463

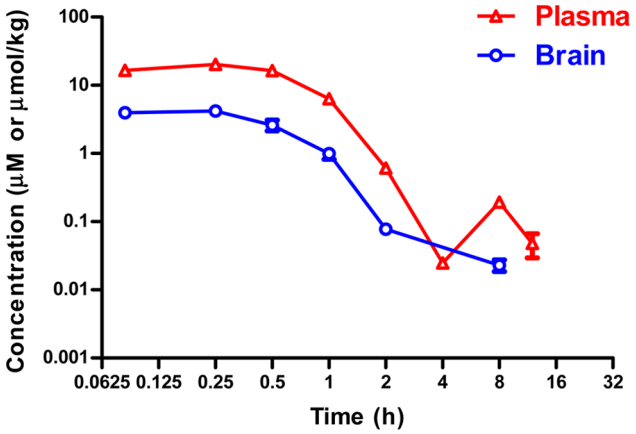

Figure 6. Mean plasma and brain concentration−time profiles of **65** after an ip dose of 30 mg/kg in male C57BL/6 mice (N = 3). The mice appeared less active at 5 min after dosing, and it lasted for about 2 h. The ip dosing solution was prepared in 10% NMP + 20% PEG 400 + 70% of 25% HP-β-CD in water. Full PK parameters are listed in the Supporting Information.

H), 7.13 (dd, J = 8.0, 1.8 Hz, 1 H), 6.61 (dd, J = 8.2, 0.8 Hz, 1 H), 5.40 (br s, 2 H); LCMS t_R = 4.25 min, m/z 290.0 [M + H$^+$]; HRMS (ESI) m/z calcd for $C_{14}H_{12}NO_4S$ [M + H$^+$] 290.0482, found 290.0486.

*11-Oxo-10,11-dihydrodibenzo[b,f][1,4]thiazepine-8-carboxylic Acid (**7**).* A solution of 3-amino-4-(2-carboxyphenylthio)benzoic acid (**6**, 4.76 g, 16.5 mmol) in THF (100 mL) was treated at 0 °C with 1,1′-carbonyldiimidazole (CDI) (10.7 g, 65.8 mmol) via several portions. The reaction mixture was warmed to room temperature and stirred at room temperature overnight. The reaction mixture was poured into 140 mL of ice−water containing concentrated HCl (20.0 mL) and stirred for 1 h. The white precipitate was filtered, washed with water, and dried to give 3.89 g (87%) of the title compound as a white solid which was used directly in the next reaction without further purification. ^{1}H NMR (400 MHz, DMSO-d_6) δ ppm 13.20 (br s, 1 H), 10.79 (s, 1 H), 7.76 (d, J = 1.2 Hz, 1 H), 7.62−7.70 (m, 3 H), 7.41−7.57 (m, 3 H); LCMS t_R = 4.55 min, m/z 271.9 [M + H$^+$]; HRMS (ESI) m/z calcd for $C_{14}H_{10}NO_3S$ [M + H$^+$] 272.0376, found 272.0376.

*Methyl 10-Methyl-11-oxo-10,11-dihydrodibenzo[b,f][1,4]-thiazepine-8-carboxylate (**8b**).* A solution of 11-oxo-10,11-dihydrodibenzo[b,f][1,4]thiazepine-8-carboxylic acid (**7**, 200 mg, 0.74 mmol) in DMF (5.00 mL) was treated at 0 °C with NaH (295 mg, 7.37 mmol). The reaction mixture was warmed to room temperature and stirred at room temperature for 1 h. Then a solution of methyl iodide (0.46 mL, 7.37 mmol) in DMF (2.00 mL) was added dropwise to the mixture. The reaction mixture was stirred at room temperature for 1.5 h. Water was carefully added, and the aqueous layer was washed with EtOAc. The aqueous layer was acidified with HCl to induce the precipitation. The precipitate was filtered, washed, and dried to give 200 mg (91%) of the title compound as a yellow solid which was used directly in the next reaction without further purification. ^{1}H NMR (400 MHz, DMSO-d_6) δ ppm 8.00 (d, J = 1.2 Hz, 1 H), 7.68−7.79 (m, 2 H), 7.59−7.66 (m, 1 H), 7.47−7.54 (m, 1 H), 7.37−7.45 (m, 2 H), 3.83 (s, 3 H), 3.52 (s, 3 H); LCMS t_R = 5.59 min, m/z 300.0 [M + H$^+$]; HRMS (ESI) m/z calcd for $C_{16}H_{14}NO_3S$ [M + H$^+$] 300.0689, found 300.0693.

*10-Methyl-11-oxo-10,11-dihydrodibenzo[b,f][1,4]thiazepine-8-carboxylic Acid (**9b**).* A solution of methyl 10-methyl-11-oxo-10,11-dihydrodibenzo[b,f][1,4]thiazepine-8-carboxylate (**8b**, 150 mg, 0.50 mmol) in THF (3.00 mL), MeOH (1.50 mL), and water (0.50 mL) was treated at room temperature with LiOH (120 mg, 5.01 mmol). The reaction mixture was stirred at room temperature for 1 h, diluted with water, and acidified with HCl. The aqueous mixture was extracted with 20% of MeOH in dichloromethane. The organic layer was separated, dried, and concentrated to give 140 mg (98%) of the title compound as a gray solid which was used directly in the next reaction without further purification. ^{1}H NMR (400 MHz, DMSO-d_6) δ ppm 13.31 (br s, 1 H), 7.98 (d, J = 1.2 Hz, 1 H), 7.67−7.76 (m, 2 H), 7.59−7.66 (m, 1 H), 7.47−7.54 (m, 1 H), 7.35−7.45 (m, 2 H), 3.52 (s, 3 H); LCMS t_R = 4.76 min, m/z 286.0 [M + H$^+$]; HRMS (ESI) m/z calcd for $C_{15}H_{12}NO_3S$ [M + H$^+$] 286.0532, found 286.0536.

*10-Methyl-11-oxo-10,11-dihydrodibenzo[b,f][1,4]thiazepine-8-carboxylic Acid 5-Oxide (**10b**).* A suspension of 10-methyl-11-oxo-10,11-dihydrodibenzo[b,f][1,4]thiazepine-8-carboxylic acid (**9b**, 660 mg, 2.31 mmol) in acetic acid (18.8 mL) was treated at room temperature with H_2O_2 (5.91 mL, 30%, 57.8 mmol) for 8 h. Upon completion, the reaction mixture was poured into a cold saturated solution of $Na_2S_2O_3$ in water and stirred at room temperature for 3 h. The mixture was then extracted with 20% of MeOH in dichloromethane. The organic layer was separated, dried, and concentrated to give 595 mg (85%) of the title compound as a white solid containing ∼5% of dioxide as a byproduct. ^{1}H NMR (400 MHz, DMSO-d_6) δ ppm 8.00 (d, J = 1.2 Hz, 1 H), 7.96 (dd, J = 8.2, 1.6 Hz, 1 H), 7.62−7.76 (m, 4 H), 7.52−7.59 (m, 1 H), 3.53 (s, 3 H); LCMS t_R = 4.02 min, m/z 302.0 [M + H$^+$]; HRMS (ESI) m/z calcd for $C_{15}H_{12}NO_4S$ [M + H$^+$] 302.0482, found 302.0486.

*10-Methyl-11-oxo-10,11-dihydrodibenzo[b,f][1,4]thiazepine-8-carboxylic Acid 5-(S)-Oxide ((S)-**10b**).* The enantiomerically pure title compound was purified to >98% purity using supercritical fluid chromatography (SFC) preparative systems at Lotus Separations, LLC (Princeton, NJ, USA). For preparative separation, an IC (2 cm × 15 cm) column was used with an eluent of 40% methanol (0.1% DEA)/CO_2, 100 bar. Flow rate was 60 mL/min, and detection wavelength was 220 nm. For analytical separation, an IC (15 cm × 0.46 cm) column was used with an eluent of 40% methanol/CO_2, 100 bar. Flow rate was 3 mL/min, and detection wavelengths were 220 and 280 nm. Retention time was 3.42 min. Retention time for the R-configuration enantiomer was 2.40 min. The material was used directly in the next coupling reaction.

*10-Methyl-11-oxo-N-(2-(thiophen-2-yl)ethyl)-10,11-dihydrodibenzo[b,f][1,4]thiazepine-8-carboxamide 5-(S)-Oxide (**65**).* A solution of 10-methyl-11-oxo-10,11-dihydrodibenzo[b,f][1,4]-thiazepine-8-carboxylic acid 5-(S)-oxide ((*S*)-**10b**, 100 mg, 0.332 mmol) in DMF (5.00 mL) was treated at room temperature with HATU (139 mg, 0.365 mmol) and diisopropylethylamine (0.174 mL, 0.996 mmol) followed by 2-(thiophen-2-yl)ethanamine (84.0 mg, 0.664 mmol). The reaction mixture was stirred at room temperature for 3 h and poured into ice−water. The white precipitate was filtered and dried to give a white solid, which was purified via silica gel chromatography using a gradient of 10−100% of EtOAc in hexanes to give 118 mg (87%) of the title compound as a white solid. ^{1}H NMR (400 MHz, DMSO-d_6) δ ppm 8.76 (t, J = 5.7 Hz, 1 H), 7.94 (d, J = 2.0 Hz, 1 H), 7.86 (dd, J = 8.2, 2.0 Hz, 1 H), 7.69−7.77 (m, 2 H), 7.67 (d, J = 8.2 Hz, 2 H), 7.51−7.60 (m, 1 H), 7.31 (dd, J = 5.1, 1.2 Hz, 1 H), 6.92 (dd, J = 5.1, 3.1 Hz, 1 H), 6.83−6.90 (m, 1 H), 3.55 (s, 3 H), 3.43−3.52 (m, 2 H), 3.02 (t, J = 7.0 Hz, 2 H); ^{13}C NMR (400 MHz, DMSO-d_6) δ ppm 165.16, 165.10, 147.66, 145.98, 141.75, 137.87, 137.02, 132.92, 131.69, 131.23, 128.20, 127.39, 126.51, 125.70, 124.57, 124.43, 121.05, 119.40, 41.55, 38.03, 29.49. LCMS retention time: t_1(method 1) = 5.348 min; t_2(method 2) = 3.188 min. HRMS (ESI) m/z (M + H)$^+$ calcd for $C_{21}H_{19}N_2O_3S_2$ [M + H$^+$] 411.0832, found 411.0831.

b. Pharmacology. For the primary screen, a calcium accumulation assay was developed using a cell line that stably expresses the D_2 DAR under the control of tetracycline (Flp-In T-REx 293, Invitogen), as well as a stably expressed chimeric G-protein (G_{qi5}) to allow coupling of the D_2 DAR to calcium release. In this system, D_2 DAR expression is induced by addition of 1 μM tetracycline to the cells prior to the assay and intracellular Ca^{2+} release is detected with a specific Ca^{2+} fluorescent dye. The resting concentration of calcium ions (Ca^{2+}) in the cytoplasm is normally maintained in the range of 10−100 nM. To maintain this low concentration, Ca^{2+} is actively pumped from the cytosol to the extracellular space and into the endoplasmic reticulum (ER) and sometimes into the mitochondria. Signaling occurs when the cell is stimulated to release Ca^{2+} from intracellular stores. The most common signaling pathway that increases cytoplasmic calcium

dx.doi.org/10.1021/jm500126s | J. Med. Chem. 2014, 57, 3450−3463

concentration is the phospholipase C (PLC) pathway. In the engineered cell line used for screening, dopamine stimulation of the D_2 DAR activates the chimeric G_{qi5} G-protein, which in turn acts on PLC which hydrolyzes the membrane phospholipid PIP2 to form inositol trisphosphate (IP3) and diacylglycerol (DAG). IP_3 diffuses to the ER, binds to its receptor (IP3 receptor), which is a Ca^{2+} channel, and thus releases Ca^{2+} from the ER to the cytosol. To measure this cytosolic Ca^{2+} accumulation, we used the Screen Quest Fluo-8 calcium assay kit (AAT Bioquest, Sunnyvale, CA). Acetoxymethyl (AM) esters bound to Fluo-8 dye are nonpolar molecules that easily cross live cell membranes transporting the dye inside the cell and are then rapidly hydrolyzed by cellular esterases inside live cells. As Fluo-8 is freed from AM esters, it binds to Ca^{2+} and emits a fluorescent signal at 514 nm that escalates with increasing cytosolic Ca^{2+}. To measure this calcium flux signal, we used the functional drug screening system (FDSS) (Hamamatsu, Japan), a high throughput screening device, which allows optical detection of signal transmissions within living cells in a time-resolving fashion.

Primary qHTS of Sytravon Library and Confirmatory Screen. D_2 Ca^{2+} Screen Assay. The cells were plated in DMEM medium with high glucose (Gibco, no. 10564), 10% FBS, 1xNEAA, and penicillin/streptomycin. At 24 h after thawing, selective antibiotics hygromycin B (10 μg/mL), puromycin (2 μg/mL), and blasticidin (15 μg/mL) were added to the medium for growing and passaging the cells. Cells were split and harvested for the experiment at ∼90% confluence with TrypLE dissociation reagent and seeded at 2100 cells, 3 μL/well in complete medium without selective antibiotics with added Tet (1 μg/mL) using a MultiDrop Combi dispenser (Thermo Scientific, Logan, UT) onto 1536-well tissue culture treated, black-walled, clear bottom plates (Greiner Bio-One North America). Quest Fluo-8 calcium reagent was freshly prepared prior to adding to the cells (lyophilized Fluo-8 dye provided with the kit was resuspended in 200 μL of DMSO as a 500× stock and stored at −20 °C). Then 2 μL/well of Quest Fluo-8 calcium dye diluted in HBSS + 10 mM HEPES buffer (for every 10 mL buffer, 1 mL of 10x quencher provided in the kit and 20 μL of 500x DMSO stock dye were added) was added to cells with a Multi-Drop Combi (ThermoScientific) and incubated for 45−90 min in the dark at ambient temperature. Then the plates were introduced into the FDSS where they were pinned with 23 nL of test compound or dopamine controls and were read by FDSS in nonstimulated mode for 180 s for detection of agonists. Compounds were tested at 2 and 10 μM (final concentrations). At that time point, 1 μL/well dopamine at 1 nM (EC_{20}) or 14 nM (EC_{80}) final concentration was added by the FDSS pipet head followed by 120 s kinetic read for detection/recording of potentiators or antagonists stimulation. The cell line HEK293 D_2 T-REx used in the primary screen was also used to confirm the activity of the active compounds selected from the primary qHTS and synthesized analogues on 1536-well format following the same protocol as described above for the primary screen. Compounds were generally tested in either 7-point titration or 12-point titrations from 5 nM to 77 μM (final concentrations).

DiscoveRx D_2 β-Arrestin Assay. For a secondary screen and selectivity assays, DAR PathHunter β-arrestin GPCR cell lines from DiscoveRx (Fremont, CA) were used. In the D_2 receptor PathHunter β-arrestin GPCR cell line, the D_2 GPCR receptor (DAR) is overexpressed and fused with a small 42-amino acid fragment of β-galactosidase called ProLink on a CHO cellular background expressing a fusion protein of β-arrestin and a larger N-terminal deletion mutant of β-galactosidase ("enzyme acceptor"). When DAR is activated by dopamine, it stimulates binding of β-arrestin to the ProLink-tagged DAR and the two complementary parts of β-galactosidase form a functional enzyme. When substrate (PathHunter detection reagent) is added, β-galactosidase hydrolyzes it and generates a chemiluminescent signal. D_2 receptor PathHunter β-arrestin cells were seeded at 2100 cells/well in 3 μL/well medium (DiscoveRx Plating Reagent 2) with MultiDrop Combi dispenser (Thermo Scientific, Logan, UT) onto white tissue culture treated 1536-well Aurora plates (Brooks Automation, Chelmsford, MA) and allowed to attach overnight at 37 °C in 5% CO_2. Next, an amount of 23 nL/well of compound solutions in DMSO was added with a pin tool transfer (Kalypsis, San Diego, CA). Compounds were generally tested in either 7-point titration or 12-point titrations from 5 nM to 77 μM (final concentrations). The cells were incubated with tested compounds for 90 min at 37 °C in 5% CO_2 and stimulated with 14 nM (EC_{80}) dopamine, after which 1.5 μL/well of DiscoveRx detection reagent was added with BioRAPTR FRD dispenser. The detection reagent was prepared by mixing of Galacton Star substrate, Emerald II solution, and PathHunter buffer (supplied by the assay kit) together at a 1:5:19 proportion just prior to dispensing. The plates were incubated at ambient temperature for 1 h, and the luminescent signal was read on a ViewLux plate reader (PerkinElmer, Waltham, MA).

Radioligand Binding Assays. Compounds were tested for differences in affinity among three dopamine receptor subtypes using radioligand binding assays. The first assay was to determine the K_i value of the compounds using the D_2 DAR subtype using stable HEK cell lines expressing the D_{2L} human dopamine receptors (Codex Biosciences, Gaithersburg, MD). Cells were cultured in Dulbecco's modified Eagle medium containing 10% FBS, 1000 units/mL penicillin, 1000 mg/mL streptomycin, 100 mM sodium pyruvate, 1 μg/mL gentamicin, and 250 mg/mL G418. All cells were maintained at 37 °C in 5% CO_2 and 90% humidity. For radioligand binding assays, cells were removed mechanically using calcium and magnesium-free Earle's balanced salt solution (EBSS(−)). Intact cells were collected by centrifugation and then lysed with 5 mM Tris-HCl and 5 mM $MgCl_2$ at pH 7.4 in a glass homogenizer. Homogenates were centrifuged at 20000g for 30 min. The membranes were resuspended in EBSS (pH 7.4) and protein concentration was determined using a Bradford assay according to the manufacturer's recommendations (Bio-Rad). Membranes were diluted to 12 μg/250 μL mixture, or 48 μg/mL. It was determined in preliminary experiments that this protein concentration gave optimal binding with minimal ligand depletion. Membrane preparations were incubated for 90 min at room temperature with various concentrations of radioligand in a reaction volume of 250 μL of EBSS containing 200 mM sodium metabisulfite. Nonspecific binding was determined in the presence of 4 μM (+)-butaclamol. Bound ligand was separated from unbound by filtration through GF/C filters using a PerkinElmer cell harvester with ice cold EBSS (four washes) and quantified on a Top-count (PerkinElmer) after addition of scintillation solution. Saturation experiments generated a K_d value of 0.2 nM and a B_{max} of ∼4200 fmol/mg for [^{3}H]methylspiperone binding to D_2 receptors. In order to determine the affinity of a given compound for a receptor type, competition-binding assays were performed. For these assays the reaction mixture was incubated with a single concentration of radiolabeled ligand (0.2 nM [^{3}H]methylspiperone) and various concentrations of competing compound. Reactions were incubated, terminated, and quantified as indicated above. K_i values of compounds were determined from observed IC_{50} values using the Cheng−Prussoff equation.

DiscoveRx D_3 β-Arrestin Assay. To determine the functional selectivity of the compounds for D_2 versus D_3 receptor antagonism, we used a D_3 PathHunter β-arrestin cell line from DiscoveRx (Fremont, CA). As for D_2, a CHO cell line was engineered to overexpress D_3 dopamine receptor (DAR) and fused with a small 42-amino acid fragment of β-gal called ProLink. In addition, these cells stably express a fusion protein of β-arrestin and a larger N-terminal deletion mutant of β-galactosidase ("enzyme acceptor"). When DAR is activated by dopamine, it stimulates binding of β-arrestin to ProLink-tagged DARs, and the two complementary parts of β-galactosidase form a functional enzyme. When substrate (PathHunter detection reagent) is added, β-galactosidase hydrolyzes it and generates a chemiluminescent signal. For the 1536-well assay, D_3 PathHunter β-arrestin cells were seeded at 2100 cells/well in 3 μL/well medium (DiscoveRx plating reagent 2) with MultiDrop Combi dispenser (Thermo Scientific, Logan, UT) onto white tissue culture treated 1536-well Aurora plates (Brooks Automation, Chelmsford, MA) and allowed to attach overnight at 37 °C in 5% CO_2. Next, an amount of 23 nL/well of compound solutions in DMSO was added with a pin tool transfer (Kalypsis, San Diego, CA). Compounds were generally tested in either 7-point titration or 12-point titrations from 5 nM to 77 μM (final concentrations). The

dx.doi.org/10.1021/jm500126s | J. Med. Chem. 2014, 57, 3450−3463

cells were incubated with tested compounds for 90 min at 37 °C in 5% CO_2 and stimulated with 14 nM (EC_{80}) dopamine, after which 1.5 μL/well of DiscoveRx detection reagent was added with BioRAPTR FRD dispenser. The detection reagent was prepared by mixing of Galacton Star substrate, Emerald II solution, and PathHunter buffer (supplied by the assay kit) together at a 1:5:19 proportion just prior to dispensing. The plates were incubated at ambient temperature for 1 h, and the luminescent signal was read on ViewLux plate reader (PerkinElmer, Waltham, MA).

D_3 Binding Assay. Compounds were counterscreened for affinity for the D_3 dopamine receptor. This was accomplished by determining the K_i values for the compounds using stable (HEK293 based) cell lines expressing the D_3 human dopamine receptors (Codex Biosciences, Gaithersburg, MD). Cells were cultured in Dulbecco's modified Eagle medium containing 10% FBS, 1000 units/mL penicillin, 1000 mg/mL streptomycin, 100 mM sodium pyruvate, 1 μg/mL gentamicin, and 250 mg/mL G418. All cells were maintained at 37 °C in 5% CO_2 and 90% humidity. For radioligand binding assays, cells were removed mechanically using calcium and magnesium-free Earle's balanced salt solution (EBSS(−)). Intact cells were collected by centrifugation and then lysed with 5 mM Tris-HCl and 5 mM $MgCl_2$ at pH 7.4 in a glass homogenizer. Homogenates were centrifuged at 20000*g* for 30 min. The membranes were resuspended in EBSS (pH 7.4), and protein concentration was determined using a Bradford assay according to the manufacturer's recommendations (Bio-Rad). Membranes were diluted to 18 μg/250 μL mixture, or 72 μg/mL, the predetermined optimal protein concentration for binding but minimal ligand depletion. Membrane preparations were incubated for 90 min at room temperature with various concentrations of radioligand in a reaction volume of 250 μL EBSS containing 200 mM sodium metabisulfite. Nonspecific binding was determined in the presence of 4 μM (+)-butaclamol. Bound ligand was separated from unbound by filtration through GF/C filters using a PerkinElmer cell harvester with ice cold EBSS (four washes) and quantified on a Topcount (PerkinElmer) after addition of scintillation solution. Saturation experiments generated a K_d value of 0.125 nM and a B_{max} of ∼600 fmol/mg for [^{3}H]methylspiperone binding to D_3 receptors. In order to determine the affinity of a given compound for a receptor type, competition-binding assays were performed. For these assays the reaction mixture was incubated with a single concentration of radiolabeled ligand (0.5 nM [^{3}H]methylspiperone) and various concentrations of competing compound. Reactions were incubated, terminated, and quantified as indicated above. K_i values of compounds were determined from observed IC_{50} values using the Cheng−Prusoff equation.

■ ASSOCIATED CONTENT

Ⓢ Supporting Information

Experimental details and spectral data of all analogues, single crystal X-ray parameters, and PK parameters for analogue **65**. This material is available free of charge via the Internet at http://pubs.acs.org.

■ AUTHOR INFORMATION

Corresponding Author

*Phone: 301-217-9198. E-mail: maruganj@mail.nih.gov.

Notes

The authors declare no competing financial interest.

■ ACKNOWLEDGMENTS

We thank Paul Shinn, Danielle van Leer, William Leister, Chris LeClair, and Heather Baker for assistance with compound purification, HRMS analysis, and compound management. We also thank Drs. Arnold L. Rheingold and Curtis Moore at the University of California, San Diego for the X-ray analysis of compounds (*R*)-**59** and **65**. This research was supported by the Molecular Libraries Initiative of the NIH Roadmap for Medical Research (Grants U54MH084681 and R21NS064831 to D.R.S.) and the Intramural Research Program of the National Center for Advancing Translational Sciences and National Institute of Neurological Disorders and Stroke, National Institutes of Health.

■ ABBREVIATIONS USED

NIH, National Institutes of Health; DAR, dopamine receptor; GPCR, G-protein-coupled receptor; CNS, central nervous system; FDA, Food and Drug Administration; RNA, ribonucleic acid; qHTS, quantitative high-throughput screening; ADME, absorption, distribution, metabolism, and excretion; MLSMR, Molecular Libraries Small Molecule Repository; BBB, blood−brain barrier; AC_{50}, compound concentration that produces half the maximal compound activity; HPLC, high-performance liquid chromatography; SAR, structure−activity relationship; SNAr, nucleophilic aromatic substitution; CDI, 1,1′-carbonyldiimidazole; MCPBA, *m*-chloroperbenzoic acid; PK, pharmacokinetics; PBS, phosphate buffered saline; ip, intraperitoneal; DMF, *N*,*N*-dimethylformamide; DMSO, dimethyl sulfoxide; TOF, time-of-flight; THF, tetrahydrofuran; SFC, supercritical fluid chromatography; DEA, diethylamine; HATU, 1-[bis(dimethylamino)methylene]-1*H*-1,2,3-triazolo[4,5-*b*]pyridinium 3-oxide hexafluorophosphate; ER, endoplasmic reticulum; PLC, phospholipase C; IP3, inositol trisphosphate; DAG, diacylglycerol; AM, acetoxymethyl; FDSS, functional drug screening system; DMEM, Dulbecco's modified Eagle medium; FBS, fetal bovine serum; HEK, human embryonic kidney cell; EBSS, Earle's balanced salt solution

■ REFERENCES

(1) Filmore, D. It's GPCR world. *Mod. Drug Discovery* **2004**, *7*, 24−28.

(2) Eglen, R. M.; Bosse, R.; Reisine, T. Emerging concepts of guanine nucleotide-binding protein-coupled receptor (GPCR) function and implications for high throughput screening. *Assay Drug Dev. Technol.* **2007**, *5*, 425−451.

(3) May, L. T.; Leach, K.; Sexton, P. M.; Christopoulos, A. Allosteric modulation of G protein-coupled receptors. *Annu. Rev. Pharmacol. Toxicol.* **2007**, *47*, 1−51.

(4) Sibley, D. R.; Monsma, F. J., Jr. Molecular biology of dopamine receptors. *Trends Pharmacol. Sci.* **1992**, *13*, 61−69.

(5) Siegel, G. J., Agranoff, B. W., Albers, R. W., Fisher, S. K., Uhler, M. D., Eds. *Basic Neurochemistry: Molecular, Cellular and Medical Aspects*, 6th ed.; Lippincott-Raven: Philadelphia, PA, 1999; pp 254−256.

(6) Callier, S.; Snapyan, M.; Le Crom, S.; Prou, D.; Vincent, J.-D.; Vernier, P. Evolution and cell biology of dopamine receptors in vertebrates. *Biol. Cell* **2003**, *95*, 489−502.

(7) (a) Lachowicz, J. E.; Sibley, D. R. Molecular characteristics of mammalian dopamine receptors. *Pharmacol. Toxicol.* **1997**, *81*, 105−113. (b) Wang, Y.; Xu, R.; Sasaoka, T.; Tonegawa, S.; Kung, M.-P.; Sankoorikal, E.-B. Dopamine D2 long receptor-deficient mice display alterations in striatum-dependent functions. *J. Neurosci.* **2000**, *20*, 8305−8314.

(8) (a) Kapur, S.; Remington, G. Dopamine D2 receptors and their role in atypical antipsychotic action: still necessary and may even be sufficient. *Biol. Psychiatry* **2001**, *50*, 873−883. (b) Beaulieu, J.-M.; Gainetdinov, R. R. The physiology, signaling, and pharmacology of dopamine receptors. *Pharmacol. Rev.* **2011**, *63*, 182−217. (c) Tandon, R.; Keshavan, M. S.; Nasrallah, H. A. Schizophrenia, "just the facts": what we know in 2008: part 1: overview. *Schizophr. Res.* **2008**, *100*, 4−19.

(9) (a) Reynolds, G. P.; Zhang, Z.-J.; Zhang, X.-B. Association of antipsychotic drug induced weight gain with a 5-HT2C receptor gene

polymorphism. *Lancet* **2002**, *359*, 2086−2087. (b) Kim, S. F.; Huang, A. S.; Snowman, A. M.; Teuscher, C.; Snyder, S. H. Antipsychotic drug-induced weight gain mediated by histamine H1 receptor-linked activation of hypothalamic AMP-kinase. *Proc. Nat. Acad. Sci. U.S.A.* **2007**, *104*, 3456−3459.

(10) Kula, N. S.; Baldessarini, R. J.; Kebabian, J. W.; Bakthavachalam, V.; Xu, L. RBI-257: a highly potent dopamine D4 receptor-selective ligand. *Eur. J. Pharmacol.* **1997**, *331*, 333−336.

(11) (a) Kalani, M. Y. S.; Vaidehi, N.; Hall, S. E.; Trabanino, R. J.; Freddolino, P. L.; Kalani, M. A.; Floriano, W. B.; Kam, V. W. T.; Goddard, W. A. The predicted 3D structure of the human D2 dopamine receptor and the binding site and binding affinities for agonists and antagonists. *Proc. Nat. Acad. Sci. U.S.A.* **2004**, *101*, 3815−3820. (b) Chien, E. Y. T.; Liu, W.; Zhao, Q.; Katritch, V.; Won Han, G.; Hanson, M. A.; Shi, L.; Newman, A. H.; Javitch, J. A.; Cherezov, V.; Stevens, R. C. Structure of the human dopamine D3 receptor in complex with a D2/D3 selective antagonist. *Science* **2010**, *330*, 1091−1095.

(12) (a) Banala, A. K.; Levy, B. A.; Khatri, S. S.; Furman, C. A.; Roof, R. A.; Mishra, Y.; Griffin, S. A.; Sibley, D. R.; Luedtke, R. R.; Newman, A. H. *N*-(3-Fluoro-4-(4-(2-methoxy or 2,3-dichlorophenyl)piperazine-1-yl)butyl)arylcarboxamides as selective dopamine D3 receptor ligands: critical role of the carboxamide linker for D3 receptor selectivity. *J. Med. Chem.* **2011**, *54*, 3581−3594. (b) Grundt, P.; Carlson, E. E.; Cao, J.; Bennett, C. J.; McElveen, E.; Taylor, M.; Luedtke, R. R.; Newman, A. H. Novel heterocyclic trans olefin analogues of *N*-{4-[4-(2,3-dichlorophenyl)piperazin-1-yl]butyl}-arylcarboxamides as selective probes with high affinity for the dopamine D3 receptor. *J. Med. Chem.* **2005**, *48*, 839−848. (c) Newman, A. H.; Grundt, P.; Cyriac, G.; Deschamps, J. R.; Taylor, M.; Kumar, R.; Ho, D.; Luedtke, R. R. *N*-(4-(4-(2,3-Dichloro- or 2-methoxyphenyl)piperazin-1-yl)butyl)heterobiarylcarboxamides with functionalized linking chains as high affinity and enantioselective D3 receptor antagonists. *J. Med. Chem.* **2009**, *52*, 2559−2570. (d) Micheli, F.; Bonanomi, G.; Blaney, F. E.; Braggio, S.; Capelli, A. M.; Checchia, A.; Curcuruto, O.; Damiani, F.; Di Fabio, R.; Donati, D.; Gentile, G.; Gribble, A.; Hamprecht, D.; Tedesco, G.; Terreni, S.; Tarsi, L.; Lightfoot, A.; Stemp, G.; MacDonald, G.; Smith, A.; Pecoraro, M.; Petrone, M.; Perini, O.; Piner, J.; Rossi, T.; Worby, A.; Pilla, M.; Valerio, E.; Griffante, C.; Mugnaini, M.; Wood, M.; Scott, C.; Andreoli, M.; Lacroix, L.; Schwarz, A.; Gozzi, A.; Bifone, A.; Ashby, C. R.; Hagan, J. J.; Heidbreder, C. 1,2,4-Triazol-3-yl-thiopropyl-tetrahydrobenzazepines: a series of potent and selective dopamine D3 receptor antagonists. *J. Med. Chem.* **2007**, *50*, 5076−5089. (e) Micheli, F.; Arista, L.; Bonanomi, G.; Blaney, F. E.; Braggio, S.; Capelli, A. M.; Checchia, A.; Damiani, F.; Di-Fabio, R.; Fontana, S.; Gentile, G.; Griffante, C.; Hamprecht, D.; Marchioro, C.; Mugnaini, M.; Piner, J.; Ratti, E.; Tedesco, G.; Tarsi, L.; Terreni, S.; Worby, A.; Ashby, C. R.; Heidbreder, C. 1,2,4-Triazolyl azabicyclo[3.1.0]hexanes: a new series of potent and selective dopamine D3 receptor antagonists. *J. Med. Chem.* **2009**, *53*, 374−391.

(13) (a) Heidbreder, C. A.; Newman, A. H. Current perspectives on selective dopamine D3 receptor antagonists as pharmacotherapeutics for addictions and related disorders. *Ann. N.Y. Acad. Sci.* **2010**, *1187*, 4−34. (b) Boeckler, F.; Gmeiner, P. Dopamine D3 receptor ligands—recent advances in the control of subtype selectivity and intrinsic activity. *Biochim. Biophy. Acta* **2007**, *1768*, 871−887.

(14) (a) Vangveravong, S.; McElveen, E.; Taylor, M.; Xu, J.; Tu, Z.; Luedtke, R. R.; Mach, R. H. Synthesis and characterization of selective dopamine D2 receptor antagonists. *Bioorg. Med. Chem.* **2006**, *14*, 815−825. (b) Grundt, P.; Husband, S. L. J.; Luedtke, R. R.; Taylor, M.; Newman, A. H. Analogues of the dopamine D2 receptor antagonist L741,626: binding, function, and SAR. *Bioorg. Med. Chem. Lett.* **2007**, *17*, 745−749. (c) Vangveravong, S.; Taylor, M.; Xu, J.; Cui, J.; Calvin, W.; Babic, S.; Luedtke, R. R.; Mach, R. H. Synthesis and characterization of selective dopamine D2 receptor antagonists. 2. Azaindole, benzofuran, and benzothiophene analogs of L-741,626. *Bioorg. Med. Chem.* **2010**, *18*, 5291−5300. (d) Langlois, X.; Megens, A.; Lavreysen, H.; Atack, J.; Cik, M.; te Riele, P.; Peeters, L.; Wouters, R.; Vermeire, J.; Hendrickx, H.; Macdonald, G.; De Bruyn, M. Pharmacology of JNJ-37822681, a specific and fast-dissociating D2 antagonist for the treatment of schizophrenia. *J. Pharmacol. Exp.Ther.* **2012**, *342*, 91−105.

(15) Bariwal, J. B.; Upadhyay, K. D.; Manvar, A. T.; Trivedi, J. C.; Singh, J. S.; Jain, K. S.; Shah, A. K. 1,5-Benzothiazepine, a versatile pharmacophore: a review. *Eur. J. Med. Chem.* **2008**, *43*, 2279−2290.

(16) (a) Ottesen, L. K.; Ek, F.; Olsson, R. Iron-catalyzed cross-coupling of imidoyl chlorides with grignard reagents. *Org. Lett.* **2006**, *8*, 1771−1773. (b) Olsson, R.; Ek, F.; Ottesen, L. K.; Bulow, A. Preparation of dibenzothiazepinecarboxamides and their analogs as cannabinoid CB1 modulators. WO2009075691A1, 2009.